

Reactivity of Lewis Acid/Base Stabilized Phosphanyl- and Arsanylboranes towards a Platinum(0) Complex

Ulf Vogel,^[a] Karl-Christian Schwan,^[a] Petra Hoemensch,^[a] and Manfred Scheer*^[a]

Dedicated to Prof. M. Meisel on the occasion of his 65th birthday

Keywords: Arsenic / Boron / Phosphorus / Reactivity / Platinum

The Lewis acid/base stabilized phosphanylboranes and -arsanes [(CO)₅W(H₂EBH₂·NMe₃)] (**1a**: E = P; **1b**: E = As) have been shown to react with the platinum(0) complex [(Ph₃P)₂-Pt(C₂H₄)] under oxidative addition of the E–H bond to the platinum center. The complexes *cis*-[(Ph₃P)₂Pt(H)(μ-EHBH₂·NMe₃)W(CO)₅] (**2a**: E = P; **2b**: E = As) are formed. Complex **2a** is unstable in solution at room temperature and slowly reacts with loss of carbon monoxide to form [(Ph₃P)₂-Pt(μ-H)(μ-EHBH₂·NMe₃)W(CO)₄] (**3a**: E = P). An analogous

complex **3b** (E = As) is formed from **2b** only by refluxing in CH₂Cl₂. The reaction of **2a** to **3a** can be reversed by addition of CO, whereas the arsenic compound **3b** does not show this reactivity pattern. All new compounds have been comprehensively characterized by spectroscopy and X-ray crystallography.

(© Wiley-VCH Verlag GmbH & Co. KGaA, 69451 Weinheim, Germany, 2005)

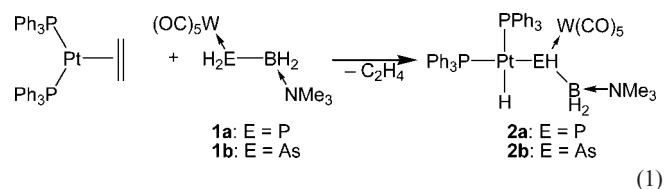
Introduction

A large number of phosphanylboranes (R₂BPR'₂)_n have been synthesized over the years,^[1] whereas only some arsanylboranes (R₂BA SR'₂)_n are known so far.^[2] Monomeric compounds of both types have up to now been stabilized exclusively by bulky substituents at the group 13 and group 15 elements. Otherwise an intermolecular oligomerisation occurs by the lone pair of the group 15 element and the acceptor orbital of the boron atom. For the experimentally unobserved parent compounds H₂BPH₂ and H₂BA SH₂ we have recently found a novel method of stabilization by the coordination of a Lewis acid and a Lewis base. Thus, the phosphanyl- and arsanylborane complexes [(CO)₅W-(EH₂BH₂·NMe₃)] (**1a**: E = P; **1b**: E = As) were synthesized by a salt elimination route starting from Li[(CO)₅WEH₂] and ClBH₂·NMe₃.^[3] Herein we report on the reactivity of **1** towards the platinum(0) complex [(Ph₃P)₂Pt(C₂H₄)] and the CO elimination/addition reactions of the products.

Results and Discussion

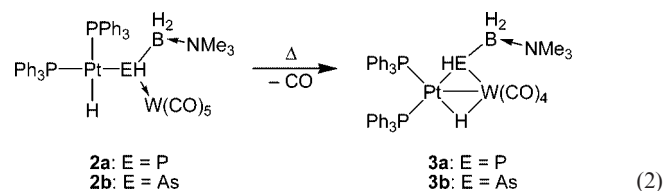
The reaction of [(CO)₅W(H₂EBH₂·NMe₃)] (**1a**: E = P; **1b**: E = As) with the platinum(0) complex [(Ph₃P)₂-Pt(C₂H₄)] at ambient temperature results in an initial oxidative addition of the platinum center to the E–H bond

of **1**, and the complexes *cis*-[(Ph₃P)₂Pt(H)(μ-EHBH₂·NMe₃)W(CO)₅] (**2a**: E = P; **2b**: E = As) are formed [Equation (1)].



(1)

For the arsenic substituted compound **2b** the reaction is complete at this stage and **2b** can be isolated as a pure compound. In contrast, even under these conditions **2a** tends to lose 1 equiv. of CO and forms the complex [(Ph₃P)₂Pt(μ-H)(μ-PHBH₂·NMe₃)W(CO)₄] (**3a**) bearing a bridging hydrogen ligand. For a full conversion the reaction mixture has to be heated to yield pure **3a** [Equation (2)]. Although pure crystalline **2a** can be isolated from the reaction (1) by fractional crystallization, if it is redissolved it tends to lose CO with formation of complex **3a**.



(2)

[a] Institut für Anorganische Chemie, Universität Regensburg
93040 Regensburg, Germany
Fax: +49-941-943-4439
E-mail: manfred.scheer@chemie.uni-regensburg.de

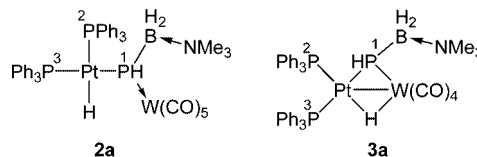
Only by heating a CH_2Cl_2 solution of the arsenic complex **2b** the formation of **3b** was detected, and the product could be isolated in pure form. Furthermore, the formation of **3a** from **2a** by loss of carbon monoxide is reversible. On saturation of a solution of **3a** with carbon monoxide, **2a** together with minor amounts of **3a** could be identified by NMR spectroscopy. In contrast, this feature has never been observed for **2b**.

Interestingly, only the diorgano-substituted phosphane complexes of the type $[(\text{CO})_5\text{M}(\text{PPh}_2\text{H})]$ show a similar reaction behavior of **1** when treated with $[(\text{C}_2\text{H}_4)\text{Pt}(\text{PPh}_3)_2]$. Here, initially the complexes *cis*- $[(\text{CO})_5\text{M}(\mu\text{-PPh}_2)\text{-Pt}(\text{H})(\text{PPh}_3)_2]$ ($\text{M} = \text{Cr}, \text{Mo}, \text{W}$) are formed, which have a strong tendency to lose CO, resulting in the compounds $[(\text{CO})_4\text{M}(\mu\text{-PPh}_2)(\mu\text{-H})\text{Pt}(\text{PPh}_3)_2]$. For these complexes the initial oxidative addition products could only be identified by NMR spectroscopy.^[4] In contrast, the complexes $[(\text{Ph}_3\text{P})_2\text{Pt}(\text{H})(\mu\text{-EH}_2)\text{W}(\text{CO})_5]$ ($\text{E} = \text{P}, \text{As}$)^[5] and $[(\text{Ph}_3\text{P})_2\text{Pt}(\text{H})(\mu\text{-PRH})\text{M}(\text{CO})_5]$ ($\text{R} = \text{Ph}, \text{cyclohexyl}; \text{M} = \text{Cr}, \text{Mo}, \text{W}$)^[6] which are structurally more closely related to **2** and are formed in a manner similar to that for **2**, both show no loss of carbon monoxide even at elevated temperatures. Thus, the occurrence of this CO loss does not seem to be caused by steric factors. Furthermore, the complexes $[(\text{Ph}_3\text{P})_2\text{Pt}(\text{H})(\mu\text{-EH}_2)\text{W}(\text{CO})_5]$ ($\text{E} = \text{P}, \text{As}$)^[5] show a *cis/trans* isomerization, whereas for **2a** and **2b** only the *cis*-addition products are detected in solution. It is interesting to note that in a related reaction of the phosphane–borane adducts $\text{PhRPH}\cdot\text{BH}_3$ ($\text{R} = \text{H}, \text{Ph}$) with $\text{Pt}(\text{PEt}_3)_3$ an oxidative addition of the P–H bond to the platinum center occurs, but in this case the *trans*-substituted complexes $[(\text{Et}_3\text{P})_2\text{Pt}(\text{H})(\text{PPhR}\cdot\text{BH}_3)]$ ($\text{R} = \text{H}, \text{Ph}$) are formed exclusively.^[7]

Complexes **2** are colorless compounds and moderately soluble in CH_2Cl_2 and toluene, whereas complexes **3** are orange crystalline complexes readily soluble in CH_2Cl_2 and toluene. In the vibrational spectra all products show bands for the CO, PH and BH functional groups. The EI mass spectra do not show the molecular ion peaks, but decomposition products including $[(\text{CO})_5\text{W}(\text{PPh}_3)]$ and $[(\text{CO})_5\text{W}(\text{H}_2\text{EBH}_2\cdot\text{NMe}_3)]$ ($\text{E} = \text{P}, \text{As}$) can be identified.

In its $^{31}\text{P}\{^1\text{H}\}$ NMR spectrum **2a** shows a signal at $\delta = -174.8$ ppm ($^1J_{\text{P1,Pt}} = 1286$, $^2J_{\text{P1,P3}} = 223$ Hz) for the P¹ atom of the phosphido group which is only slightly shifted to lower field when compared with free **1a** ($\delta = -184.2$ ppm). The signal is very broad because of the quadrupolar moment of the neighboring boron atom, which is directly bound to the phosphorus atom. Upon recording a $^{31}\text{P}\{^{11}\text{B}, ^1\text{H}\}$ NMR spectrum, the coupling to the tungsten atom and to the P² atom *cis* to P¹ (see Scheme 1) is also revealed ($^2J_{\text{P1,P2}} = 11$, $^1J_{\text{P1,W}} = 153$ Hz). The P² atom shows a pseudo-triplet at $\delta = 29.4$ ppm ($^1J_{\text{P2,Pt}} = 2099$, $^2J_{\text{P2,P1}} = 11$, $^2J_{\text{P2,P3}} = 14$ Hz) and P³ is detected as a doublet of doublets at $\delta = 25.9$ ppm ($^1J_{\text{P3,Pt}} = 2199$, $^2J_{\text{P3,P2}} = 14$, $^2J_{\text{P3,P1}} = 223$ Hz). This coupling pattern clearly shows the *cis* arrangement of the phosphanidoboranyl ligand relative to the hydrido ligand. The latter ligand is detected in the ^1H NMR spectrum of **2a** as a doublet of doublets of doublets at $\delta = -4.48$ ppm showing platinum satellites. The PH proton

appears as a doublet at $\delta = 2.38$ ppm. A signal for the BH_2 protons could not be assigned, as this resonance is too broad to be clearly identified from the background in the spectrum.



Scheme 1.

Complex **3a** shows a similar $^{31}\text{P}\{^1\text{H}\}$ NMR spectrum, which is depicted in Figure 1. Here, the P¹ atom shows a broad doublet at $\delta = -8.7$ ppm. Upon additional boron decoupling the signal shows a doublet of doublets bearing platinum satellites. The large downfield shift of the signal compared to **2a** can be explained by the bridging position of the phosphidoboranyl ligand.^[8] Also the phosphorus–platinum coupling constant (951 Hz) is much smaller than in **2a** (1286 Hz). A coupling to the tungsten atom is not obvious, but it is presumably hidden under the main signals. Signals for the P² and P³ atoms appear at $\delta = 15.7$ and 19.5 ppm, respectively, and show the same coupling pattern as in **2a**. In its ^1H NMR spectrum **3a** shows a doublet of doublets with platinum satellites at $\delta = -7.43$ ppm (Figure 1). Due to the small intensity of the hydride signals, the expected tungsten satellites cannot be clearly differentiated from the background noise. The resonance for the PH protons appears as a doublet at $\delta = 2.60$ ppm. As in the case for **2a** the BH_2 signal for **3a** could not be detected.

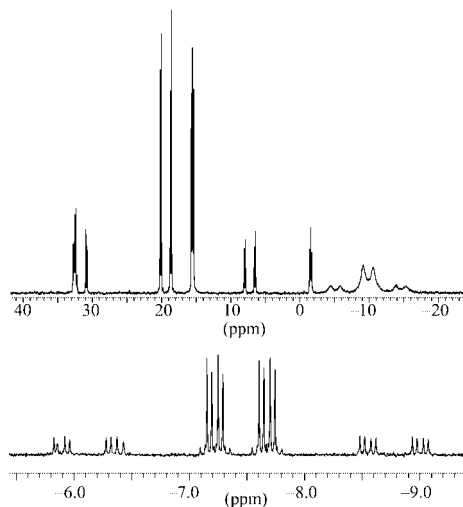
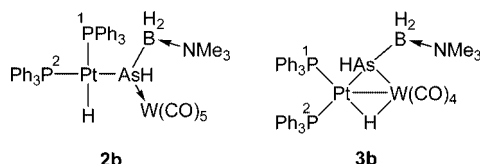


Figure 1. $^{31}\text{P}\{^1\text{H}\}$ NMR spectrum of **3a** (top). Hydride region of the ^1H NMR spectrum of **3a** (bottom).

The $^{31}\text{P}\{^1\text{H}\}$ NMR spectrum of compound **2b** (Scheme 2) shows two doublets at $\delta = 30.7$ ppm and 23.6 ppm, both bearing platinum satellites ($^2J_{\text{P1,P2}} = 13$, $^1J_{\text{P1,Pt}} = 2145$ Hz, $^1J_{\text{P2,Pt}} = 2531$ Hz). In its ^1H NMR spectrum **2b** displays a doublet of doublets at $\delta = -4.76$ ppm with platinum satellites for the hydrido ligand bound to the platinum atom ($^2J_{\text{H,P1}} = 177$, $^2J_{\text{H,P2}} = 19$ Hz). In accord-

ance with the $^{31}\text{P}\{^1\text{H}\}$ NMR spectrum this coupling pattern shows the *cis* arrangement of the phosphane ligands around the platinum center. In the ^1H NMR spectrum the protons bound to the arsenic atom give rise to a complex signal centered at $\delta = -1.27$ ppm.



Scheme 2.

In the $^{31}\text{P}\{^1\text{H}\}$ NMR spectrum complex **3b** (Scheme 2) shows two doublets with platinum satellites at $\delta = 15.2$ ppm and 16.9 ppm ($^2J_{\text{P1,P2}} = 16$, $^1J_{\text{P1,Pt}} = 2657$, $^1J_{\text{P2,Pt}} = 3433$ Hz) for both non-equivalent phosphorus atoms. The ^1H NMR spectrum of **3b** shows the same characteristic signals as that of complex **3a**. The hydrido ligand bound to the platinum atom gives rise to a doublet of doublets with platinum satellites at $\delta = -6.74$ ppm ($^2J_{\text{H,P1}} = 116$, $^2J_{\text{H,P2}} = 24$, $^1J_{\text{H,Pt}} = 669$ Hz). Signals for the nine protons of the trimethylamine group and the 30 protons of the phenyl groups are detected at $\delta = 1.95$ ppm and 6.8–7.6 ppm, respectively.

In order to confirm the proposed structures of **2** and **3** X-ray crystal structure determinations have been performed on all compounds. Single crystals of complex **2** could be obtained from CH_2Cl_2 solutions. Whereas **2b** crystallizes as a dichloromethane solvate, for **2a** no solvent molecule was found in the unit cell. As an example the molecular structure of **2a** is depicted in Figure 2; in Table 1 the bond lengths and angles are compared.

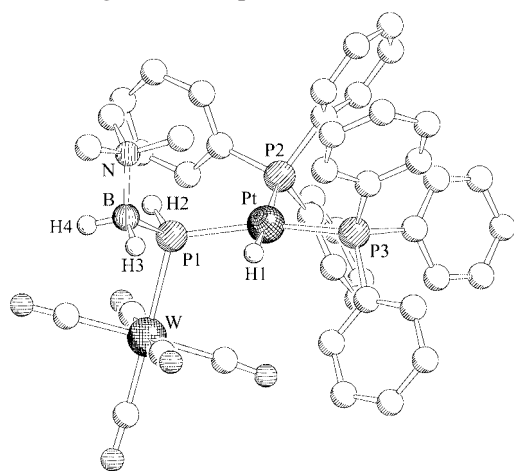


Figure 2. Molecular structure of **2a** in the crystal. Hydrogen atoms at the carbon atoms are omitted for clarity.

The key structural feature of **2** is a central platinum atom which shows an almost perfect planar coordination sphere. Two phenylphosphane ligands are in *cis* arrangement to each other. A hydride and the phosphanidoboranyl or arsanidoboranyl ligand (**2a** or **2b**) complete the coordination sphere of the 16-electron complexes. The sum of the bond angles around the platinum atom are close to 360° [**2a**:

Table 1. Comparison of selected bond lengths [pm] and angles $^\circ$] in **2a** and **2b**.

Bond lengths ^[a]	2a	2b
Pt–E	233.0(2)	243.6(1)
Pt–P _{cis}	233.1(1)	232.1(2)
Pt–P _{trans}	231.0(2)	229.9(2)
E–W	260.5(1)	270.2(1)
E–B	198.1(6)	209.4(9)
B–N	161.8(7)	162(1)
Angles	2a	2b
E–Pt–P _{cis}	98.29(5)	100.06(5)
E–Pt–P _{trans}	159.71(5)	157.60(5)
P _{cis} –Pt–P _{trans}	101.87(5)	101.35(7)
Pt–E–W	111.20(5)	112.07(3)
Pt–E–B	118.1(3)	116.0(3)
W–E–B	106.1(2)	106.3(3)
E–B–N	116.4(4)	115.2(6)

[a] **2a**: E = P1, P_{cis} = P2, P_{trans} = P3; **2b**: E = As, P_{cis} = P1, P_{trans} = P2.

359.87(5) $^\circ$; **2b**: 359.01(7) $^\circ$]. Despite the planar coordination around the platinum atom the bond angles are far from 90° required for a square-planar coordination. All ligands are shifted towards the hydride ligand to alleviate steric crowding. The Pt–P bond lengths in both compounds are comparable and in a range usually found for such bonds. In comparison to the starting material the B–E [**1a**: 195.5(4); **2a**: 198.1(6); **1b**: 206.7(9); **2b**: 209.4(9) pm] and the E–W bonds [**1a**: 254.2(2); **2a**: 260.5(1); **1b**: 263.5(1); **2b**: 270.15(8) pm] are elongated.^[3] The elongation of the E–W bond can be explained by the back-bonding of the E atom to two metal atoms instead of one metal atom as in compound **1**. The same effect can be observed for $[(\text{CO})_5\text{W}(\mu\text{-PH}_2)\text{PtH}(\text{PPh}_3)_2]$ [W–P 260.3(3) pm] in comparison to $[(\text{CO})_5\text{-WPH}_3]$ [W–P 249.1(2) pm].^[5] The change of the electron density at the E atom in **2** and **3** can also explain the elongation of the E–B bond.

The compounds **3a** and **3b** are isostructural and crystallize in the triclinic space group $P\bar{1}$ as the dichloromethane solvates. As an example the molecular structure of **3a** is depicted in Figure 3; in Table 2 the bond lengths and angles are compared.

The essential feature of the structures is a $(\text{CO})_4\text{-WPt}(\text{PPh}_3)_2$ moiety which is bridged by a hydride ligand and a phosphanidoboranyl and an arsanidoboranyl ligand (**3a** or **3b**), respectively. Like in the compounds **2** the platinum atoms show a nearly planar coordination geometry [sum of bond angles **3a**: 357.74(7) $^\circ$; **3b**: 357.49(7) $^\circ$]. The long distance between the platinum and the tungsten atom [**3a**: 302.8(1); **3b**: 307.72(9) pm] implies indirect multi-centered bonding through the bridging ligands, rather than a direct metal–metal bond, as was discussed for the structurally related compound $[(\text{CO})_4\text{Cr}(\mu\text{-PPh}_2)(\mu\text{-H})\text{Pt}(\text{PEt}_3)_2]$.^[4b] The E–B distances [**3a**: 197.5(8); **3b**: 207.3(8) pm] are comparable to **2a** and **2b**, respectively. In comparison to **2a** and **2b**, respectively, the E–W bond lengths in **3a** and **3b** are significantly reduced [**3a**: 246.0(1); **3b**: 255.57(9) pm] but in a range normally found for similar complexes $\{[(\text{CO})_4\text{-}$

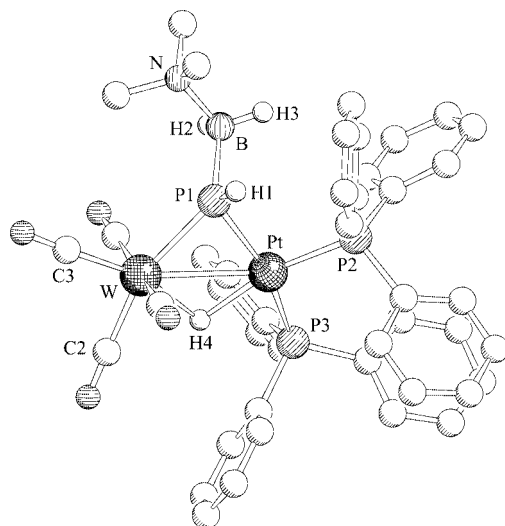


Figure 3. Molecular structure of **3a** in the crystal. Hydrogen atoms at the carbon atoms are omitted for clarity.

Table 2. Comparison of selected bond lengths [pm] and angles [°] of **3a** and **3b**.

Bond lengths ^[a]	3a	3b
Pt–E	233.7(2)	245.1(1)
Pt–P _{cis}	228.5(2)	229.0(2)
Pt–P _{trans}	232.3(2)	231.0(2)
Pt–W	302.8(1)	307.7(1)
E–W	246.0(2)	255.6(1)
E–B	197.5(8)	207.3(8)
B–N	162(1)	161(1)
W–C2	199.6(8)	200.6(8)
W–C3	194.9(8)	195.1(8)
Angles	3a	3b
E–Pt–P _{cis}	95.18(7)	94.89(6)
E–Pt–P _{trans}	159.79(6)	159.50(5)
P _{cis} –Pt–W	144.09(5)	144.90(5)
P _{cis} –Pt–P _{trans}	102.77(7)	103.10(7)
P _{trans} –Pt–W	111.97(5)	110.96(5)
E–Pt–W	52.68(5)	53.63(3)
W–E–B	125.48(5)	125.44(5)
E–B–N	111.04(7)	111.58(6)

[a] **3a**: E = P1, P_{cis} = P2, P_{trans} = P3; **3b**: E = As, P_{cis} = P1, P_{trans} = P2.

W(μ-PPh₂)₂Pt(MeO₂CC≡CCO₂Me): W–P: 244.3(3) and 243.5(3) pm}.^[9]

Conclusions

The results have shown that the Lewis acid/base stabilized phosphanylborane and arsanylborane undergo oxidative addition reactions at a Pt⁰ center only at the P–H bond. Initially we had expected that the B–H bond also shows some addition behavior, as it is known for Rh and Ir complexes.^[10] However, the boranyl substituent in **1** only functions as an electron-withdrawing substituent at the group 15 atom. Furthermore, in comparison to organo-substituted PH-containing phosphanes, the boranyl-substituted complexes **1** show a similar reaction behaviour toward Pt⁰

centers. Oxidative addition of the E–H bond leads to exclusive formation of *cis*-substituted Pt^{II} complexes, which can lose CO to form a complex with a bridging hydrido and pnicoenido substituent, respectively.

Experimental Section

General Remarks: All manipulations were carried out under dinitrogen using standard Schlenk techniques. All solvents were dried using standard procedures and distilled freshly before use. [(CO)₅W(H₂EBH₂·NMe₃)] (**1a**: E = P; **1b**: E = As)^[3] and [(Ph₃P)₂Pt(C₂H₄)]^[11] were prepared according to the literature. All NMR spectra were recorded with a Bruker AC 250 with δ referenced to external SiMe₄ (¹H), F₃B·OEt₂ (¹¹B) or H₃PO₄ (³¹P), respectively. IR spectra were measured with a Bruker IFS-28, Raman spectra with a Bruker FRA 106 spectrometer. All mass spectra were recorded with a Varian MATR 711.

cis-[(Ph₃P)₂Pt(H)(μ-PHBH₂·NMe₃)W(CO)₅] (**2a**): A mixture of [W(CO)₅(H₂PBH₂·NMe₃)] (**1a**) (467 mg, 1.09 mmol) and [(C₂H₄)Pt(PPh₃)₂] (814 mg, 1.09 mmol) was stirred in toluene (20 mL) at room temperature for 14 h. The solution turned to an orange color during this time and a yellow precipitate was formed. The precipitate was separated by filtration and dissolved in a minimum amount of CH₂Cl₂ (ca. 4–5 mL). After 2 d, **2a** was obtained at 4 °C as colorless crystals (if the solution is too concentrated, orange crystals of **3a** crystallize additionally). Yield: 638 mg (51%). C₄₄H₄₃BNO₅P₃PtW (1148.45): calcd. C 46.02, H 3.77, N 1.22; found C 46.23, H 3.87, N 1.14. Raman (solid state) $\tilde{\nu}$ = 3061 (vs), 3006 (w), 2949 (w), 2370 (w), 2295 (w), 2048 (s), 1951 (vs), 1895 (m), 1873 (s), 1518 (s), 1573 (m), 1097 (m), 1029 (m), 1002 (vs), 789 (w), 461 (m), 439 (m), 260 (w), 174 (w), 114 (s) cm⁻¹. ¹H NMR (250 MHz, CD₂Cl₂): δ = −4.48 (ddd, ¹J_{Pt,H} = 971, ²J_{P,H} = 176, ²J_{P,H} = 33, ²J_{P,H} = 22 Hz, 1 H, HPt), 2.38 (m, ¹J_{P,H} ≈ 300 Hz, 1 H, PH), 2.49 (s, 9 H, NMe₃), 7.0–7.5 (m, 30 H, PPh₃) ppm. ³¹P{¹H} NMR (101 MHz, CD₂Cl₂): δ = −174.8 (br. d, ²J_{P,P} = 223, ¹J_{Pt,P} = 1286 Hz, PHBH₂), 25.9 (dd, ²J_{P,P} = 223, ²J_{P,P} = 14, ¹J_{Pt,P} = 2199 Hz, PPh₃), 29.4 (t, ²J_{P,P} = 14, ¹J_{Pt,P} = 2099 Hz, PPh₃) ppm. ³¹P{¹¹B, ¹H} NMR (101 MHz, CD₂Cl₂): δ = −174.8 (dd, ²J_{P,P} = 11 Hz ²J_{P,P} = 223, ¹J_{W,P} = 153, ¹J_{Pt,P} = 1286 Hz, PHBH₂), 25.9 (dd, ²J_{P,P} = 223, ²J_{P,P} = 14, ¹J_{Pt,P} = 2199 Hz, PPh₃), 29.4 (t, ²J_{P,P} = 14, ¹J_{Pt,P} = 2099 Hz, PPh₃) ppm. EI-MS (170 °C): *m/z* (%) = 586 (16) [W(CO)₅PPh₃]⁺, 558 (4) [W(CO)₄PPh₃]⁺, 530 (2) [W(CO)₃PPh₃]⁺, 502 (93) [W(CO)₂PPh₃]⁺, 474 (1) [W(CO)PPh₃]⁺, 446 (100) [WPh₃]⁺, 429 (22) [(CO)₅WPh₂BH₂NMe₃]⁺, 401 (11) [(CO)₄WPh₂BH₂NMe₃]⁺, 373 (14) [(CO)₃WPh₂BH₂NMe₃]⁺, 370 (50) [(CO)₅WPh₂BH₂]⁺, 345 (6) [(CO)₂WPh₂BH₂NMe₃]⁺, 342 (31) [(CO)₄WPh₂BH₂]⁺, 317 (4) [(CO)WPh₂BH₂NMe₃]⁺, 314 (15) [(CO)₃WPh₂BH₂]⁺, 286 (10) [(CO)₂WPh₂BH₂]⁺, 262 (89) [PPh₃]⁺.

cis-[(Ph₃P)₂Pt(H)(μ-AsHBH₂·NMe₃)W(CO)₅] (**2b**): A mixture of [W(CO)₅(H₂AsBH₂·NMe₃)] (**1b**) (75 mg, 0.16 mmol) and [(C₂H₄)Pt(PPh₃)₂] (119 mg, 0.16 mmol) was stirred in toluene (10 mL) at room temperature for 16 h. During this time the orange solution turned to a yellow suspension. The precipitate was separated by filtration and dissolved in a minimum amount of CH₂Cl₂ (3–4 mL). The resulting solution was stored at −25 °C. After 2 d, **2b** was obtained as colorless crystals. Yield: 134 mg (70%). C₄₄H₄₃AsBNO₅P₂PtW·0.5CH₂Cl₂ (1234.87): calcd. C 43.28, H 3.59, N 1.13; found C 43.43, H 3.32, N 1.28. Raman (solid state) $\tilde{\nu}$ = 3060 (vs), 3006 (w), 2948 (w), 2093 (w), 2046 (s), 1951 (vs), 1874 (s), 1858 (w), 1587 (vs), 1574 (m), 1158 (w), 1096 (m), 1029 (s), 1002 (vs), 465 (m), 439 (m), 259 (w), 205 (w), 175 (w), 110 (s) cm⁻¹. ¹H NMR (250 MHz, CD₂Cl₂): δ = −4.95 (dd, ²J_{P,H} = 177,

$^2J_{\text{P,H}} = 19$, $^1J_{\text{P,H}} = 904$ Hz, 1 H, HPT), -1.27 (m, 2 H, AsH_2), 2.48 (s, 9 H, NMe_3), 7.11–7.29 (m, 30 H, PPh_3) ppm. $^{31}\text{P}\{^1\text{H}\}$ NMR (101 MHz, CD_2Cl_2): $\delta = 23.6$ (d, $^2J_{\text{P,P}} = 13$, $^1J_{\text{P,P}} = 2531$ Hz, PPh_3), 30.7 (d, $^2J_{\text{P,P}} = 13$, $^1J_{\text{P,P}} = 2145$ Hz, PPh_3) ppm. ^{31}P NMR (101 MHz, CD_2Cl_2): $\delta = 23.6$ (s, 1 P, PPh_3), 30.7 (d, $^2J_{\text{H,P}} = 177$ Hz, PPh_3). EI-MS (200 °C): m/z (%) = 586 (15) $[(\text{CO})_5\text{WPPH}_3]^+$, 558 (16) $[(\text{CO})_4\text{WPPH}_3]^+$, 530 (3) $[(\text{CO})_3\text{WPPH}_3]^+$, 502 (70) $[(\text{CO})_2\text{WPPH}_3]^+$, 446 (67) $[\text{WPPH}_3]^+$, 445 (35) $[(\text{CO})_4\text{WAsH}_2\text{BH}_2\cdot\text{NMe}_3]^+$, 262 (100) $[\text{PPh}_3]^+$.

[(Ph₃P)₂Pt(μ-H)(μ-PHBH₂·NMe₃)W(CO)₄] (3a): A mixture of $[\text{W}(\text{CO})_5(\text{H}_2\text{PBH}_2\cdot\text{NMe}_3)]$ (**1a**) (467 mg, 1.09 mmol) and $[(\text{C}_2\text{H}_4)\text{Pt}(\text{PPh}_3)_2]$ (814 mg, 1.09 mmol) was stirred in toluene (20 mL) at room temperature for 14 h. The solution turned to an orange color during this time and a yellow precipitate was formed. The precipitate was separated by filtration and dissolved in CH_2Cl_2 (10 mL). The resulting solution was heated under reflux for 6 h while a slow stream of nitrogen was passed through the apparatus. Reduction of the solvent to a volume of ca. 2 mL and storage at 4 °C yielded **3a** as orange crystals. Yield: 733 mg (60%). $\text{C}_{43}\text{H}_{43}\text{BNO}_4\text{P}_3\text{PtW}\cdot 0.5\text{CH}_2\text{Cl}_2$ (1162.91): calcd. C 44.93, H 3.81, N 1.20; found C 44.84, H 3.72, N 1.08. Raman (solid state): $\tilde{\nu} = 3058$ (vs), 3004 (w), 2943 (w), 2392 (w), 2291 (m), 2050 (m), 1987 (m), 1956 (s), 1861 (s), 1821 (w), 1586 (s), 1482 (m, br), 1096 (m), 1028 (m), 1001 (vs), 704 (w), 496 (m), 436 (m), 116 (s) cm^{-1} . ^1H NMR (250 MHz, CD_2Cl_2): $\delta = -7.43$ (ddd, $^1J_{\text{P,H}} = 664$, $^2J_{\text{P,H}} = 113$, $^2J_{\text{P,H}} = 24$, $^2J_{\text{P,H}} = 10$ Hz, 1 H, HPT), 2.60 (m, $^1J_{\text{P,H}} = 287$ Hz, 1 H, PH), 2.45 (s, 9 H, NMe_3), 7.0–7.5 (m, 30 H, PPh_3) ppm. $^{31}\text{P}\{^1\text{H}\}$ NMR (101 MHz, CD_2Cl_2): $\delta = -8.7$ (br. d, $^2J_{\text{P,P}} = 147$, $^1J_{\text{P,P}} = 951$ Hz, PHBH_2), 15.7 (t, $^2J_{\text{P,P}} = 17$, $^1J_{\text{P,P}} = 3462$ Hz, PPh_3), 19.5 (dd, $^2J_{\text{P,P}} = 147$, $^2J_{\text{P,P}} = 17$, $^1J_{\text{P,P}} = 2463$ Hz, PPh_3) ppm. $^{31}\text{P}\{^{11}\text{B}, ^1\text{H}\}$ NMR (101 MHz, CD_2Cl_2): $\delta = -8.7$ (dd, $^2J_{\text{P,P}} = 15$, $^2J_{\text{P,P}} = 147$, $^1J_{\text{P,P}} = 951$ Hz, PHBH_2), 15.7 (t, $^2J_{\text{P,P}} = 17$, $^1J_{\text{P,P}} = 3462$ Hz, PPh_3), 19.5 (dd, $^2J_{\text{P,P}} = 147$, $^2J_{\text{P,P}} = 17$, $^1J_{\text{P,P}} = 2463$ Hz, PPh_3) ppm. EI-MS (90 °C) $m/z = 586$ (6) $[\text{W}(\text{CO})_5\text{PPh}_3]^+$, 558 (8) $[\text{W}(\text{CO})_4\text{PPh}_3]^+$, 530 (1) $[\text{W}(\text{CO})_3\text{PPh}_3]^+$, 502 (22) $[\text{W}(\text{CO})_2\text{PPh}_3]^+$, 474 (1) $[\text{W}(\text{CO})\text{PPh}_3]^+$, 446 (19) $[\text{WPPH}_3]^+$, 429 (19) $[(\text{CO})_5\text{WPH}_2\text{BH}_2\text{NMe}_3]^+$, 401 (6) $[(\text{CO})_4\text{WPH}_2\text{BH}_2\text{NMe}_3]^+$, 373 (6) $[(\text{CO})_3\text{WPH}_2\text{BH}_2\text{NMe}_3]^+$, 370 (16) $[(\text{CO})_5\text{WPH}_2\text{BH}_2]^+$, 345 (2) $[(\text{CO})_2\text{WPH}_2\text{BH}_2\text{NMe}_3]^+$, 342 (13) $[(\text{CO})_4\text{WPH}_2\text{BH}_2]^+$, 317 (3) $[(\text{CO})\text{WPH}_2\text{BH}_2\text{NMe}_3]^+$, 314 (6) $[(\text{CO})_3\text{WPH}_2\text{BH}_2]^+$, 286 (3) $[(\text{CO})_2\text{WPH}_2\text{BH}_2]^+$, 262 (100) $[\text{PPh}_3]^+$.

[(Ph₃P)₂Pt(μ-H)(μ-AsHBH₂·NMe₃)W(CO)₄] (3b): Complex **2b** (70 mg, 0.059 mmol) was dissolved in CH_2Cl_2 (15 mL) and refluxed for 12 h which led to a color change from yellow to orange. Reduction of the volume of the solution to ca. 2 mL and storage at -25 °C yielded **3b** as orange crystals. Yield: 41 mg (60%). $\text{C}_{43}\text{H}_{43}\text{AsBNO}_4\text{P}_2\text{PtW}\cdot 0.5\text{CH}_2\text{Cl}_2$ (1206.86): calcd. C 43.29, H 3.67, N 1.16; found C 43.46, H 3.50, N 1.29. Raman (solid state): $\tilde{\nu} = 3054$ (vs), 2380 (w), 2294 (w), 2092 (m), 2051 (m), 2031 (s), 1962 (w), 1860(b), 1586 (s), 1185 (w), 1160 (w), 1095 (m), 1028 (m), 1001 (vs), 773 (w), 703 (w), 475 (m), 437 (m), 172 (w), 113 (s) cm^{-1} . ^1H NMR (250 MHz, C_6D_6): $\delta = -6.74$ (dd, $^2J_{\text{P,H}} = 116$, $^2J_{\text{P,H}} = 24$, $^1J_{\text{P,H}} = 669$ Hz, 1 H, HPT), 0.32 (s, 1 H, AsH), 1.95 (s, 9 H, NMe_3), 6.8–7.6 (m, 30 H, PPh_3) ppm. $^{31}\text{P}\{^1\text{H}\}$ NMR (101 MHz, C_6D_6): $\delta = 15.2$ (d, $^2J_{\text{P,P}} = 16$, $^1J_{\text{P,P}} = 3433$ Hz, PPh_3), 16.9 (d, $^2J_{\text{P,P}} = 16$, $^1J_{\text{P,P}} = 2657$ Hz, PPh_3) ppm. ^{31}P NMR (101 MHz, C_6D_6): $\delta = 15.2$ (d, $^2J_{\text{H,P}} = 123$ Hz, PPh_3), 16.9 (s, PPh_3) ppm. EI-MS (200 °C): $m/z = 586$ (20) $[(\text{CO})_5\text{WPPH}_3]^+$, 558 (16) $[(\text{CO})_4\text{WPPH}_3]^+$, 530 (3) $[(\text{CO})_3\text{WPPH}_3]^+$, 502 (70) $[(\text{CO})_2\text{WPPH}_3]^+$, 446 (67) $[\text{WPPH}_3]^+$, 445 (35) $[(\text{CO})_4\text{WAsH}_2\text{BH}_2\cdot\text{NMe}_3]^+$, 262 (100) $[\text{PPh}_3]^+$.

X-ray Crystallographic Study: Data were collected with a STOE IPDS area-detector diffractometer using $\text{Ag-K}\alpha$ ($\lambda = 0.56087$ Å) radiation. Machine parameters, crystal data and data collection parameters are summarized in Table 3. The structures were solved by direct methods using SHELXS-97,^[12a] full-matrix-least-squares

Table 3. Crystallographic data for **2a,b** and **3a,b**.

	2a	2b ·0.5CH ₂ Cl ₂	3a ·0.5CH ₂ Cl ₂	3b ·0.5CH ₂ Cl ₂
Empirical formula	C ₄₄ H ₄₃ BNO ₅ P ₃ PtW	C _{44.5} H ₄₄ AsBCINO ₅ P ₂ PtW	C _{43.5} H ₄₄ BCINO ₄ P ₃ PtW	C _{43.5} H ₄₄ AsBCINO ₄ P ₂ PtW
<i>M_r</i>	1148.45	1234.87	1162.91	1206.86
<i>T</i> [K]	203(2)	203(2)	203(2)	203(2)
Crystal size	0.20 × 0.20 × 0.06	0.18 × 0.12 × 0.03	0.20 × 0.10 × 0.04	0.25 × 0.15 × 0.10
Space group	<i>Pbcn</i>	<i>P2₁/c</i>	<i>P</i> $\bar{1}$	<i>P</i> $\bar{1}$
Crystal system	orthorhombic	monoclinic	triclinic	triclinic
<i>a</i> [Å]	20.017(4)	14.891(3)	10.661(2)	10.774(2)
<i>b</i> [Å]	24.139(5)	18.897(3)	12.458(3)	12.490(3)
<i>c</i> [Å]	18.389(4)	18.195(3)	18.995(4)	18.976(4)
α [°]	90	90	82.06(3)	81.72(3)
β [°]	90	108.06(3)	76.89(3)	76.18(3)
γ [°]	90	90	71.84(3)	71.67(3)
<i>V</i> [Å ³]	8885(3)	4867.7(15)	2328.5(8)	2347.2(8)
<i>Z</i>	8	4	2	2
<i>d_c</i> [g cm ⁻³]	1.717	1.685	1.659	1.708
μ_c [mm ⁻¹]	3.185	3.275	3.066	3.393
2θ range [°]	2.72–41.82	3.40–42.00	3.60–45.00	3.12–44.78
<i>hkl</i> range	$-23 \leq h \leq 24$ $-16 \leq k \leq 29$ $-23 \leq l \leq 23$	$-19 \leq h \leq 18$ $-24 \leq k \leq 24$ $-21 \leq l \leq 23$	$-14 \leq h \leq 14$ $-16 \leq k \leq 16$ $-25 \leq l \leq 25$	$-14 \leq h \leq 14$ $-16 \leq k \leq 16$ $-23 \leq l \leq 24$
Data/restraints/parameters	7960/0/524	10245/0/547	11790/0/528	11591/2/533
No. of unique data	7960 (<i>R</i> _{int} = 0.0501)	10245 (<i>R</i> _{int} = 0.0653)	11790 (<i>R</i> _{int} = 0.0464)	11591 (<i>R</i> _{int} = 0.0519)
Independent reflections [<i>I</i> > 2σ(<i>I</i>)]	6127	7547	8543	8300
Goodness-of fit on <i>F</i> ²	1.008	1.040	1.022	0.997
<i>R</i> ₁ ^[a] , <i>wR</i> ₂ ^[b] [<i>I</i> > 2 σ(<i>I</i>)]	0.0309, 0.0671	0.0415, 0.0953	0.0426, 0.1027	0.0447, 0.1053
<i>R</i> ₁ ^[a] , <i>wR</i> ₂ ^[b] [all data]	0.0492, 0.0731	0.0690, 0.1059	0.0702, 0.1156	0.0724, 0.1176
Largest diff. peak/hole [e·Å ⁻³]	0.611, -0.554	2.015, -0.823	2.238, -1.527	3.172, -1.127

[a] $R = \sum |F_o| - |F_c| / \sum |F_o|$. [b] $wR_2 = [\sum w(F_o^2 - F_c^2)^2] / [\sum (F_o^2)^3]^{0.5}$.

refinement on F^2 in SHELXL-97^[12b] with anisotropic displacement for non-H atoms, hydrogen atoms placed in idealized positions and refined isotropically according to the riding model. The H atoms at the heavy atoms were found as residue electron densities and could be freely refined except for the H atom at the As atom in **2b**, which was placed in an idealized position. The use of restraints was necessary for the refinement of **3b** to fix the Cl atoms at the solvent molecule in appropriate distances. CCDC-249065 to -249068 (**2a,b** and **3a,b**) contain the supplementary crystallographic data for this paper. These data can be obtained free of charge from The Cambridge Crystallographic Data Centre via www.ccdc.cam.ac.uk/data_request/cif.

Acknowledgments

This work was comprehensively supported by the Deutsche Forschungsgemeinschaft and the Fonds der Chemischen Industrie. The authors thank the Degussa and Umicore AG for the gift of precious metal compounds.

- [1] For a review see: R. T. Paine, H. Nöth, *Chem. Rev.* **1995**, *95*, 343–379.
- [2] Compare: a) M. S. Lube, R. L. Wells, P. S. White, *Main Group Met. Chem.* **1996**, *13*, 733–741; b) M. A. Mardones, A. H. Cowley, L. Contreras, R. A. Jones, C. J. Carrano, *J. Organomet. Chem.* **1993**, *455*, C1–C2; c) M. A. Petrie, M. M. Olmstead, H. Hope, R. A. Bartlett, P. P. Power, *J. Am. Chem. Soc.* **1993**, *115*, 3221–3226; d) R. Goetze, H. Nöth, *Z. Naturforsch.* **1975**, *30B*, 875–882.
- [3] U. Vogel, P. Hoemensch, K.-C. Schwan, A. Y. Timoshkin, M. Scheer, *Chem. Eur. J.* **2003**, *9*, 515–519.
- [4] a) J. Powell, M. R. Gregg, J. F. Sawyer, *J. Chem. Soc., Chem. Commun.* **1984**, 1149–1150; b) J. Powell, M. R. Gregg, J. F. Sawyer, *Inorg. Chem.* **1989**, *28*, 4451–4460.
- [5] U. Vogel, M. Scheer, *Z. Anorg. Allg. Chem.* **2001**, *627*, 1593–1598.
- [6] J. Schwald, P. Peringer, *J. Organomet. Chem.* **1987**, *323*, C51–C53.
- [7] C. A. Jaska, H. Dorn, A. J. Lough, I. Manners, *Chem. Eur. J.* **2003**, *9*, 271–281.
- [8] P. E. Garrou, *Chem. Rev.* **1981**, *81*, 229–266.
- [9] E. D. Morrison, A. D. Harley, M. A. Marcelli, G. L. Geoffroy, A. L. Rheingold, W. C. Fultz, *Organometallics* **1984**, *3*, 1407–1413.
- [10] For recent reviews see: a) H. Braunschweig, M. Colling, *Coord. Chem. Rev.* **2001**, *223*, 1–51; b) H. Braunschweig, *Angew. Chem.* **1998**, *110*, 1882–1898; *Angew. Chem. Int. Ed. Engl.* **1998**, *37*, 1786–1801; c) G. J. Irvine, M. J. G. Lesley, T. B. Marder, N. C. Norman, C. R. Rice, E. G. Robins, W. R. Roper, G. R. Whittell, L. J. Wright, *Chem. Rev.* **1998**, *98*, 2685–2722.
- [11] U. Nagel, *Chem. Ber.* **1982**, *115*, 1998–1999.
- [12] a) G. M. Sheldrick, *SHELXS-97*, University of Göttingen, **1997**; b) G. M. Sheldrick, *SHELXL-97*, University of Göttingen, **1997**.

Received: October 7, 2004